Tuning of betatron radiation in laser-plasma accelerators via multimodal laser propagation through capillary waveguides

A. Curcio, D. Giulietti, and M. Petrarca

Citation: Phys. Plasmas **24**, 023104 (2017); doi: 10.1063/1.4975185
View online: http://dx.doi.org/10.1063/1.4975185
View Table of Contents: http://aip.scitation.org/toc/php/24/2
Published by the American Institute of Physics

Tuning of betatron radiation in laser-plasma accelerators via multimodal laser propagation through capillary waveguides

A. Curcio,[1,2] D. Giulietti,[3] and M. Petrarca[4]
[1]*INFN-LNF, via Enrico Fermi 40, 00044 Frascati (Rome), Italy*
[2]*Department of Physics, "Sapienza" University of Rome, Piazzale A. Moro 2, I-00185 Rome, Italy*
[3]*Physics Department, University of Pisa and INFN, Largo Bruno Pontecorvo 3, 56127 Pisa, Italy*
[4]*Department of Basic and Applied Sciences for Engineering (SBAI) and INFN-Roma1, "Sapienza" University of Rome, Via A. Scarpa 14, 00161 Rome, Italy*

(Received 27 November 2016; accepted 17 January 2017; published online 6 February 2017)

The betatron radiation from laser-plasma accelerated electrons in dielectric capillary waveguides is investigated. The multimode laser propagation is responsible for a modulated plasma wakefield structure, which affects the electron transverse dynamics, therefore influencing the betatron radiation spectra. Such a phenomenon can be exploited to tune the energy spectrum of the betatron radiation by controlling the excitation of the capillary modes. *Published by AIP Publishing.* [http://dx.doi.org/10.1063/1.4975185]

I. INTRODUCTION

Innovative acceleration techniques based on wakefields induced by ultrashort lasers propagating in underdense plasmas are actually suitable for the realization of compact bright X-ray secondary sources.[1–8] The use of a capillary waveguide filled with plasma[9–14] is particularly important as a solution to increase the laser plasma interaction region by guiding the laser intensity over many Rayleigh lengths and accelerate electrons to very high energies.[15] The modal structure imposed by the boundary conditions of the capillary affects the laser dynamics and consequently the plasma response to the laser pulse, which is a fundamental characteristic of the system to be taken into consideration in order to design and perform acceleration experiments, for example, the external injection.[16] In this scheme, an electron bunch must be injected on the right phase of the wakefield to undergo an acceleration as if it was in a conventional LINAC structure. In the present work, a numerical fluid model[17] is exploited to characterize the plasma response to the laser pulse excitation along the capillary. It is shown that the multimodal propagation of the laser reveals itself in the beating among the propagating modes imposed by the capillary structure. This effect produces a modulated structure of the wakefield affecting the electron plasma dynamics and therefore the characteristics of the emitted betatron radiation. The calculated wakefields are used to track the trajectories of single electrons of an externally injected electron bunch. Finally, by starting from the calculated electron trajectories, the betatron spectrum of the radiation is evaluated. The electron dynamics is studied in different cases of multimodal laser propagation. The differences in the emitted betatron spectra are pointed out, revealing the possibility to correlate specific mode-mixture of the laser inside the capillary to specific frequency tuning of the betatron spectra.

II. BRIEF DESCRIPTION OF THE LASER PROPAGATION MODEL

We refer to the propagation model of Ref. 17. The propagation of a laser pulse in a dielectric capillary gives rise to a modal structure, coupling a linearly polarized laser, impinging at the entrance of a capillary waveguide, to the so called hybrid modes. The general equation governing the propagation of a linearly polarized laser pulse inside a plasma medium along the z axis is[11]

$$\Box a = \left(\frac{1}{c^2}\frac{\partial^2}{\partial t^2} - \frac{\partial^2}{\partial z^2} - \nabla_\perp^2\right) a = -k_{p0}^2 \frac{n_e}{\gamma n_0} a, \qquad (1)$$

where the Lorentz factor is[11] $\gamma(r,z,t) = \sqrt{1 + a(r,z,t)^2/2}$, $a = eA/mc$ is the normalized vector potential, e is the electron charge, A is the modulus of the laser vector potential, m is electron mass, c is the speed of light in vacuum, k_{p0} is the plasma wavenumber corresponding to the background density n_0, and n_e is the plasma electron density. The boundary conditions are dictated by the continuity of the electromagnetic field components at the capillary walls and are the same of Ref. 9. Let us denote with $a_n = a_n(r)a_n(z,t)$ the hybrid mode of order n, which is a solution of the vacuum homogeneous equation $\Box a_n = 0$. In Table I, the quantities of interest are listed, where a_{n0} is the initial normalized vector potential amplitude of the nth mode, r is the radial coordinate in cylindric symmetry, ε_r is the relative dielectric constant, R_{cap} is the capillary radius, k_0 and ω_0 are the laser wave number and pulsation, respectively, τ is the laser pulse duration parameter, J_0 is the zero order Bessel function of the first kind, and u_n the nth zero of J_0.

The coupling efficiency of a flat top profile laser focused into a vacuum capillary is given by

$$C_m = \frac{4}{J_1^2(u_m)}\left|\int_0^1 J_1\left(\frac{\nu_2 R_{cap} x}{r_0}\right) J_0(u_m x)dx\right|^2, \qquad (2)$$

where r_0 is the focus radius defined at the second zero $\nu_2 = 7.0156$ of J_1. This assumption is required by the fact that high power lasers have a flat-top radial beam profile on the focusing element giving a bessel-like structure at focus. From Fig. 1, the maximum coupling efficiency is obtained

TABLE I. The quantities of interest for the hybrid modes of order n.

Normalized vector potential	$a_n(r,z,t) \sim a_{n0} J_0(u_n r/R_{cap}) \exp[-k_n^l z + i(\omega_0 t - k_{zn} z) - (z - v_{g,n} t)^2/2c^2\tau^2]$
Damping coefficient	$k_n^l = u_n^2(1+\varepsilon_r)/2k_{zn}^2 R_{cap}^3(\varepsilon_r - 1)^{1/2}$
Longitudinal wave number	$k_{zn} = (k_0^2 - u_n^2/R_{cap}^2)^{1/2}$
Transverse wave number	$k_{\perp n} = u_n/R_{cap}$
Group velocity of mode nth	$v_{g,n} = c(1 - (k_{\perp n}/k_0)^2)^{1/2}$

for $R_{cap}/r_0 \sim 0.5$, resulting in 83% of the laser energy coupled to the EH_{11} mode and in the damping of the secondary lobe on the wall of the capillary entrance surface. The general solution of (1) in vacuum is $a = \sum_n c_n a_n$, where c_n are constant coefficients determined by the initial conditions. As in Ref. 17, we expand the solution of the inhomogeneous equation on the basis functions a_n, letting the expansion coefficients varying in (z, t) coordinates. From now on, $c_n \equiv c_n(z,t)$.

Using the homogeneous equation and expressing $a = \sum_n c_n(z,t) a_n$, Equation (1) becomes

$$\Box a + \hat{P} a = \sum_n a_n \Box c_n(z,t) + \hat{P} a_n c_n(z,t) = 0, \quad (3)$$

where we defined the plasma operator $\hat{P} = k_{p0}^2 n_e/\gamma n_0$. After performing straightforward algebra and under the assumptions $\omega_0 \tau \gg 1$ and $L_{cap}|(1/v_{g,n} - 1/v_{g,m})|/\tau \ll 1$ with L_{cap} the length of the capillary and $k_{p0} \gg \Delta k_{nm}, k_n^l$, the following final equation in the co-moving frame (ζ, t), where $\zeta = z - v_g t$ and $v_g = v_{g,1}$ is the group velocity of the fundamental mode is obtained:

$$\left[\frac{\partial^2}{c^2 \partial t^2} - \frac{2}{c}\frac{\partial^2}{\partial \zeta \partial t}\right] c_n(\zeta,t) + \frac{1}{a_{n0}^2}\sum_m P_{nm}(\zeta,t) c_m(\zeta,t) = 0. \quad (4)$$

The assumptions made above correspond, respectively, to slowly varying envelope approximation of the laser pulse, to a negligible longitudinal modal dispersion (the different modes do not separate along the propagation path) and to the choice of an electron plasma density such that the beating frequency is much lower than the plasma frequency. In the linear regime $a < 1$, the plasma electron density perturbation driven by the laser pulse is[11]

$$\Delta n_e = \frac{n_0 c^2}{2\omega_{p0}} \int_0^t dt' \sin[\omega_{p0}(t - t')] \nabla^2 a^2. \quad (5)$$

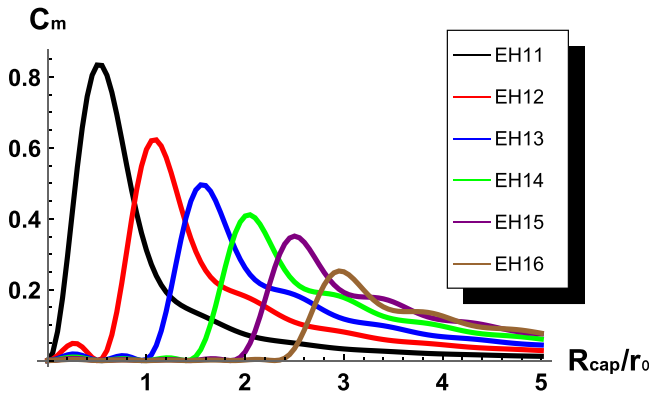

FIG. 1. The coupling efficiency coefficients for a flat top profile laser focused into a dielectric capillary tube.

The plasma operator can be expressed in a more explicit form in the following way:

$$\frac{P_{nm}}{k_{p0}^2} = \left\langle a_n \left| \frac{1}{\gamma} + \frac{c^2}{2\gamma\omega_{p0}} \int_0^t dt' \sin[\omega_{p0}(t-t')] \right. \right. \times \nabla^2 \left(\sum_n c_n a_n \right)^2 \left| a_m \right\rangle, \quad (6)$$

where the product $P_{nm} = \langle a_n | \hat{P} | a_m \rangle$ is defined as[17]

$$\langle a_n | \hat{P} | a_m \rangle \sim 2 a_{n0} a_{m0} e^{-\frac{(z - v_{g,n} t)^2}{c^2 \tau^2}} \frac{\int_0^1 dx J_0(u_n x) x \hat{P} J_0(u_m x)}{J_1^2(u_m)}. \quad (7)$$

For our calculations, we focus on the following parameters: capillary radius $R_{cap} = 60\,\mu$m, capillary length $L_{cap} = 5$ cm, and dielectric relative constant (for the glass type of the capillary) $\varepsilon_r = 2.25$. A background electron plasma density of $n_0 = 10^{17}\,\text{cm}^{-3}$ is considered, and consequently, the gaussian laser pulse temporal duration $\tau \sim \sqrt{2}/\omega_p$ is fixed to be resonant with the plasma density.[18] In this paragraph, we report calculations of the laser-driven plasma density perturbation based on initial conditions for the coupling coefficients at the entrance of the capillary corresponding to $R_{cap}/r_0 = 0.5$, 1, 1.5, 2, 2.5, 3, according to Fig. 1. In other words, different initial matching configurations of the laser into the capillary are considered. These conditions allow to couple the laser energy in such a way that an effective initial normalized vector potential value at the entrance of the capillary of $a_0 \sim 0.8$ is obtained for each matching configuration, taking into account of the total laser intensity distributed among the different modes. The initial matching of the laser pulse to the capillary is then slightly modified also by the interaction with the plasma, including the scattering with the laser-produced electron plasma wave and the self-channeling effects.[17] In Figs. 2–7 the modulated amplitude of the wakefields generated by the laser pulse propagating through the totally preionized gas (we consider hydrogen) is reported for the initial matching configurations $R_{cap}/r_0 = 0.5$, 1, 1.5, 2, 2.5, 3. As shown in Ref. 17, the electron plasma wave in the case of the capillary guided laser propagation can be expressed as $\Delta n_e = \delta n_e(z,r) \sin(k_{p0}\zeta)$, where $\delta n_e(z, r)$ is the plasma wave amplitude modulated along the capillary $(z = v_g t)$.

Even in the case of perfect matching of the laser pulse inside the capillary in vacuum, i.e., when only the fundamental mode is expected propagating in vacuum, if the laser pulse propagates through an underdense plasma exciting an electron plasma wave, this in turn can excite higher modes, determining a complex structure of the wakefields. The controlled excitation of higher modes, performed with a specific

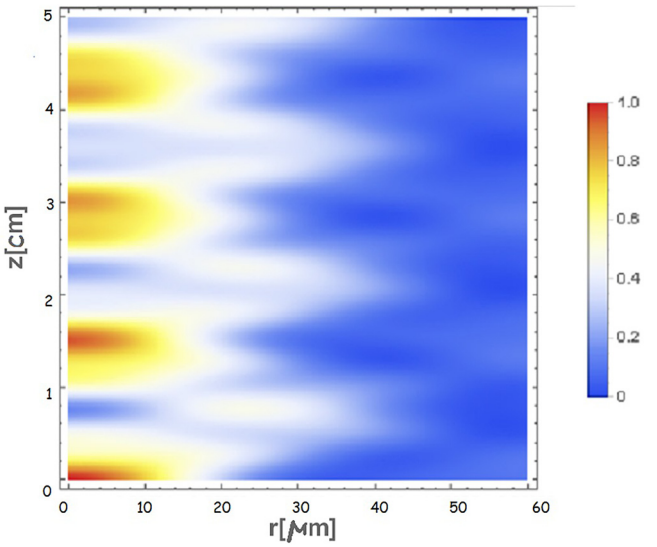

FIG. 2. 2D map of the plasma wave amplitude $\delta n_e(z, r)$ (normalized to the maximum value) modulations along the capillary generated by a guided laser pulse propagating through a preionized gas for the initial matching condition $R_{cap}/r_0 = 0.5$ according to Fig. 1.

choice of the background plasma density and of the initial matching configuration, can allow to set specific amplitudes for the single excited modes inside the waveguide in order to create controlled modulations of the plasma wave amplitude. In the next part of the present paper, we are going to study the dynamics of electrons which are externally injected in the laser-generated structured wakefields described in the present section, then studying the effects on the betatron radiation spectra.

III. ELECTRON DYNAMICS AND BETATRON RADIATION

Once the wakefields are determined by the propagation model described in Sec. II, the dynamics of externally

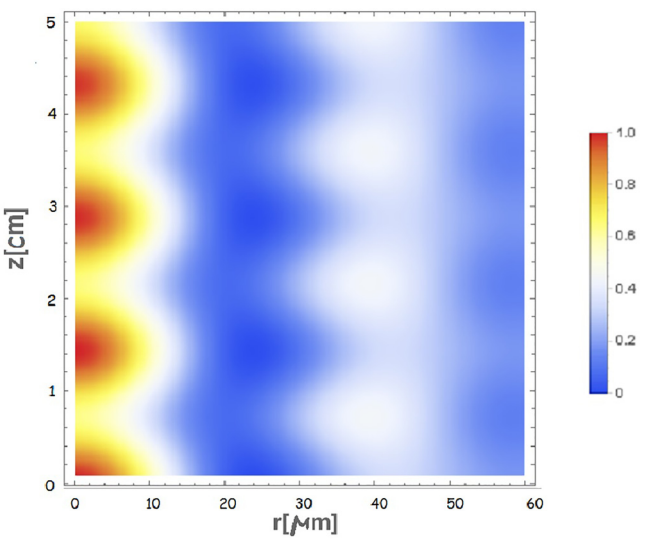

FIG. 3. 2D map of the plasma wave amplitude $\delta n_e(z, r)$ (normalized to the maximum value) modulations along the capillary generated by a guided laser pulse propagating through a preionized gas for the initial matching condition $R_{cap}/r_0 = 1$ according to Fig. 1.

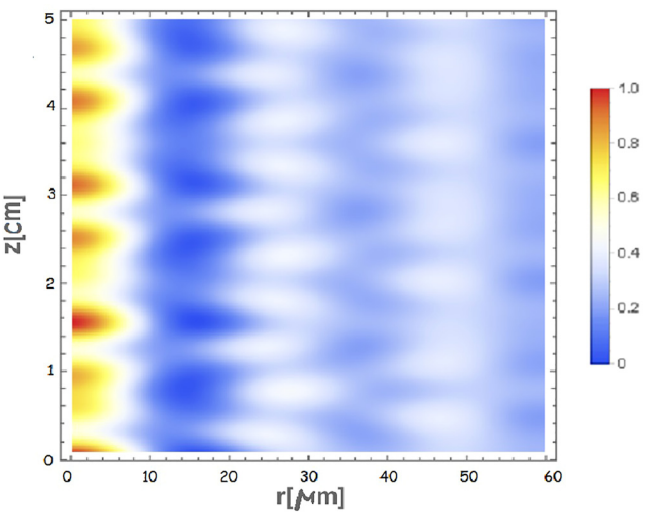

FIG. 4. 2D map of the plasma wave amplitude $\delta n_e(z, r)$ (normalized to the maximum value) modulations along the capillary generated by a guided laser pulse propagating through a preionized gas for the initial matching condition $R_{cap}/r_0 = 1.5$ according to Fig. 1.

injected electrons can be studied. The equation of motion for an electron accelerating and oscillating inside a plasma wakefield structure is

$$\frac{d\gamma\vec{r}}{dt} = -\frac{e}{m}\vec{E_W}, \tag{8}$$

where E_W is the wakefield, related to the electron plasma perturbation by the Poisson equation $\varepsilon_0\vec{\nabla}\cdot\vec{E_W} = -e\Delta n_e$. Being the wake field related to the gradient of the normalized laser intensity $\vec{\nabla}a^2$, which in the capillary is decomposed in normal modes $a^2 = (\sum_n a_n)^2$, the net force acting on the electrons will consist of many terms related to the driving force offered by pure modes (proportional to a_n^2) and that offered by beating modes (proportional to $a_n a_m$ terms with $m \neq n$). We are going to study in particular, the transverse dynamics

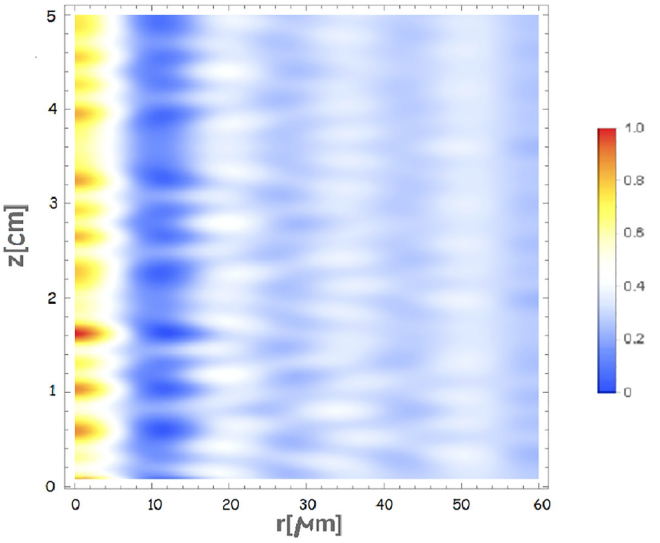

FIG. 5. 2D map of the plasma wave amplitude $\delta n_e(z, r)$ (normalized to the maximum value) modulations along the capillary generated by a guided laser pulse propagating through a preionized gas for the initial matching condition $R_{cap}/r_0 = 2$ according to Fig. 1.

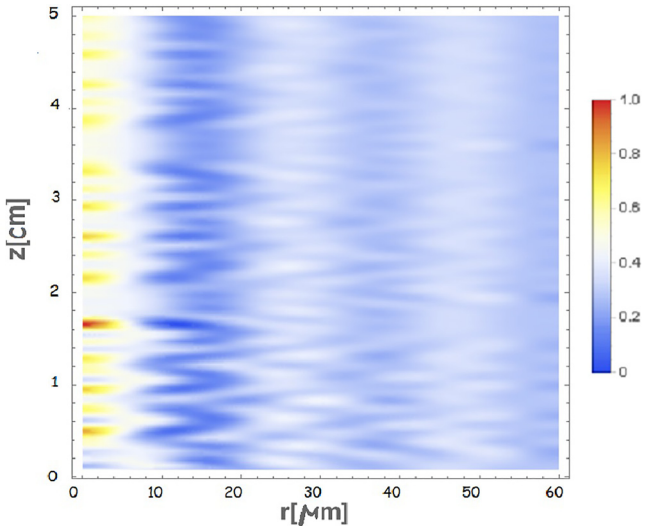

FIG. 6. 2D map of the plasma wave amplitude $\delta n_e(z, r)$ (normalized to the maximum value) modulations along the capillary generated by a guided laser pulse propagating through a preionized gas for the initial matching condition $R_{cap}/r_0 = 2.5$ according to Fig. 1.

of single electrons under the action of complex structured wakefields, due to the multimodal propagation of a laser pulse inside a capillary waveguide. Referring to the same parameters for laser intensity (at the entrance of the capillary), plasma density and capillary characteristics specified in Sec. II we want to point out the differences in the betatron oscillation dynamics for different configurations of the laser coupling into the capillary. For our simulations, we choose six working points for the initial matching of the laser into the capillary, namely, by referring to Fig. 1, we choose a six initial configurations with $R_{cap}/r_0 = 0.5$, 1, 1.5, 2, 2.5, 3. The betatron oscillations relative to the first two configurations present strong amplitude modulations, determining a blueshift of the radiation spectrum (Fig. 8). Then, the modulations start to decrease because the average laser intensity

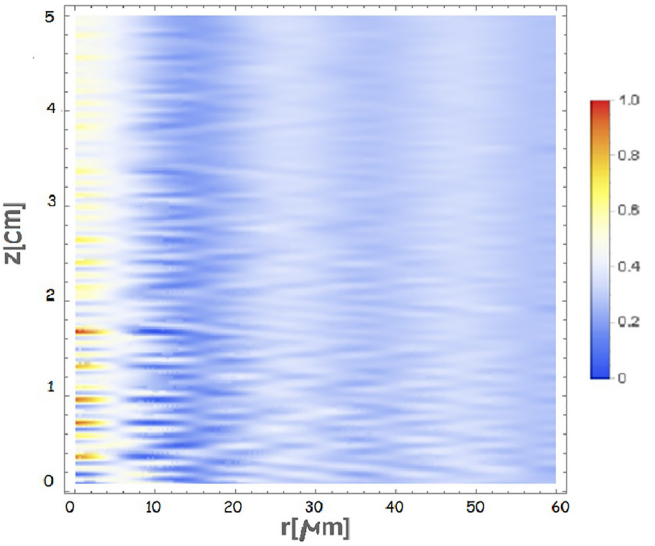

FIG. 7. 2D map of the plasma wave amplitude $\delta n_e(z, r)$ (normalized to the maximum value) modulations along the capillary generated by a guided laser pulse propagating through a preionized gas for the initial matching condition $R_{cap}/r_0 = 3$ according to Fig. 1.

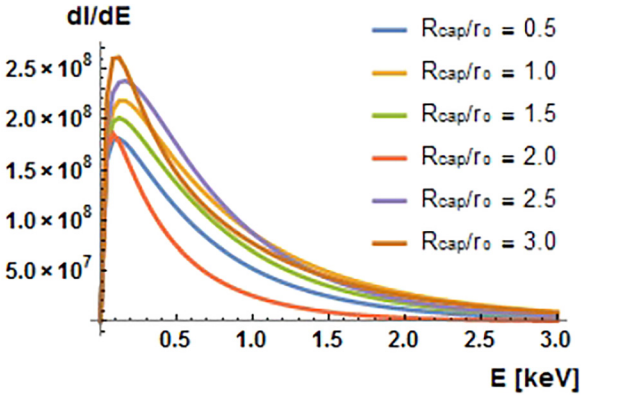

FIG. 8. Spectrum comparison for different initial matching configurations of the laser into the waveguide ($R_{cap}/r_0 = 0.5$, 1, 1.5, 2, 2.5, 3).

actually decreases for matching conditions such that $R_{cap}/r_0 > 1$. Nevertheless the betatron oscillation amplitudes start to be effectively modulated again when $R_{cap}/r_0 > 2$ because the beating frequencies Δk_{45} and Δk_{56}, which are effective in the case of initial matching with $R_{cap}/r_0 > 2$, are comparable (they start to resonate) with the proper betatron frequency of the system, so inducing a growth[19,20] of the electron betatron oscillation amplitude. The tuning curve of the critical energy at the plasma background density $n_0 = 10^{17}\,\mathrm{cm}^{-3}$ and for a laser and a capillary as described above is reported in Fig. 9, obtained with a polynomial fit based on the critical energy values extracted from the spectra of Fig. 8. The critical energy is defined as the photon energy of the spectrum which separates half of the radiated energy below its value while half above. The radiation spectra in Fig. 8 are calculated by considering an externally injected gaussian electron bunch with rms beam size $\sigma_r = 2\,\mu$m, relative energy spread $\delta\gamma/\gamma = 0.005$, rms time duration $\sigma_t = 50$ fs, charge $Q = 50$ pC, injection energy $\sim mc^2 k_0/k_{p0} \sim 65$ MeV, and energy gain $\sim$510 MeV. We do not consider laser-plasma accelerated electron beams for the external injection, but, for example, electron beams coming from high-brightness photo-injectors with typical duration of tens of femtoseconds. By the way, electron beams with even shorter duration on the scale of few femtoseconds (like those produced in typical laser-plasma acceleration experiments) would be only better in

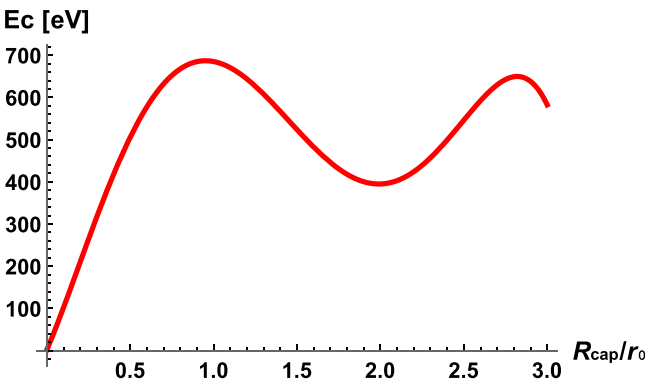

FIG. 9. Tuning curve of the critical energy relative to the betatron radiation spectra at the plasma background density $n_0 = 10^{17}\,\mathrm{cm}^{-3}$ for different initial matching conditions between the laser spot size and the capillary radius.

terms of the accumulated energy spread, which is proportional, at the first order, to the product $\omega_p\sigma_\tau$. In fact, the shorter is the electron bunch duration with respect to the plasma period the less important is the energy spread accumulated during the acceleration. The trajectories are evaluated for ten thousand test electrons of the bunch experiencing the wakefields calculated with the propagation code introduced in Sec. II. In Ref. 21, formulas for the radiation emitted by an accelerated charge in arbitrary motion are reported in the special case when the divergence of the emitting bunch is much greater than the natural aperture of the cone of the emitted radiation. This corresponds to the physical conditions of our interest. The divergence of the electron bunch whose electrons undergo betatron oscillations is evaluated as K_β/γ, where the betatron strength parameter $K_\beta = \gamma\sigma_r k_\beta$ is related to the rms transverse size of the bunch σ_r, to the average electron energy γ and to the betatron wavenumber k_β. The natural divergence of the radiation is $1/\gamma$. The condition for the applicability of the radiation formula (9)[21] becomes $K_\beta \gg 1$, which is the wiggler condition. The radiation cone is dominated by the divergence of the electron beam K_β/γ

$$\frac{dI}{dE} = -\frac{2\alpha E}{\sqrt{\pi}\hbar}\int_0^{L_{cap}/c}\frac{dt}{\gamma^2(t)}\left[\frac{\Phi'(u)}{u} + \frac{1}{2}\int_{-\infty}^{\infty} du\Phi(u)\right], \quad (9)$$

where $\Phi(u)$ is the Airy function of first kind where we defined

$$u = \left(\frac{2E}{\hbar c k_{p0}^2 x(t)\gamma^2(t)}\right). \quad (10)$$

dI is the differential radiated energy, α the fine structure constant, $x(t)$ is the transverse coordinate of the electron undergoing betatron oscillations, and E the energy of the radiated photon. The calculated critical energies fall in the soft X-rays region, where interesting applications in fundamental physics can be found; therefore, the possibility to finely tune the emitted radiation could be an important tool in this kind of experiments. The self-injection of electron beams from the rear of the wakefields is not considered in this paper because the regime which is studied is linear ($a < 1$), while the self-injection is a strongly non-linear phenomenon which occurs at higher local laser intensities. The propagation code which is used by the authors takes also into account the self-focusing phenomena; nevertheless at this laser intensity level and for this order of electron plasma density, they are not important, ensuring the preservation of the linear regime of interaction over the whole capillary, excluding the possibility of self-injected electron beams and consequently the emitted betatron radiation. By looking at Equation (6), which describes the interaction via the electron plasma wave among the various laser modes propagating through the capillary, we can see that the interaction does not depend directly on the background electron plasma density n_0, while it depends on the value of a_0 and on the degree of resonance of excitation of the plasma wave, controlled by the parameter $\omega_p\tau$. Therefore, when considering different values of n_0, while keeping the same value of $a_0 = 0.8$ and the optimal value (for a gaussian laser pulse) of the product $\omega_p\tau \sim \sqrt{2}$, the changes in the plasma structure are only local, in the sense that the plasma oscillations change frequency, higher for higher densities, but the structure of the beatings among the modes is conserved. The changes in the betatron radiation are described by Equation (11). The critical energy depends on the background electron plasma density both directly and through the term γ^2. In particular, the γ^2 term is dominant and the critical energy decreases with the increase in n_0. By performing simulations considering new values $n_0 = 3, 7 \times 10^{17}\,\mathrm{cm}^{-3}$, the tuning curves at different n_0 look like in Fig. 10.

We choose as maximum value $n_0 = 7 \times 10^{17}\,\mathrm{cm}^{-3}$ because it corresponds to a dephasing length $L_{deph} = \omega_0^2\lambda_p/2\omega_p^2 \sim 5\,\mathrm{cm}$, which is the capillary length. We are not interested in greater values of n_0 because at higher densities the dephasing length is shorter than the capillary length, which is not an optimal condition for the final energy gain. The difference among the critical energy values relative to the different laser modal structures in the waveguide seems to be rather important, paving the possibility to finely tune the X-ray radiation over a wide frequency band.

IV. GENERAL DISCUSSIONS

The scaling of the critical energy with respect to the electron energy and to the background electron plasma density is

$$E_c \propto T\left(\frac{R_{cap}}{r_0}\right)\gamma^2 n_0\sigma_r, \quad (11)$$

where $T(R_{cap}/r_0)$ is proportional to the tuning function of Fig. 9. From Equation (11), we obtain

$$\frac{dE_c}{E_c} \sim 2\frac{d\gamma}{\gamma} + \frac{dn_0}{n_0} + \frac{d\sigma_r}{\sigma_r} + \frac{d(R_{cap}/r_0)}{(R_{cap}/r_0)}. \quad (12)$$

Equation (12) states that if the electron energy spread, the background electron plasma density and the electron beam size are shot-to-shot well-controlled quantities, the tuning effect related to the last term in 12 is effective, and the curve in Fig. 9 is the real tuning curve of the radiation source. In realistic experimental conditions for an electron external injection experimental setup, we can consider that the energy spread, the background electron plasma density, and the

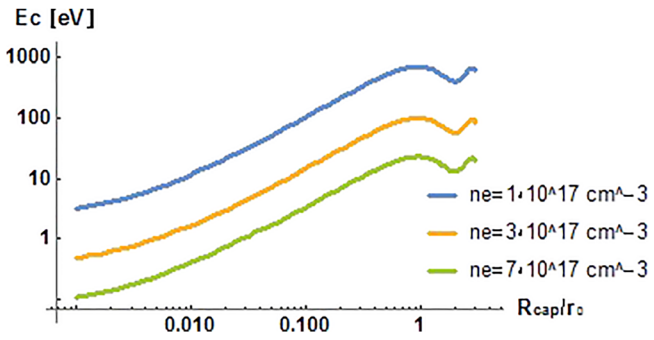

FIG. 10. The tuning curves of the critical energy related to the betatron radiation spectra at different background electron plasma densities.

beam size are quantity controlled at the percent level. The energy spread value we chose for our simulations $d\gamma/\gamma = 0.005$ is a pretty good value compared to what commonly is obtained in laser-plasma acceleration experiments. Nevertheless in the present paper, the external injection of good quality electron beams is treated. The aim is that to inject a good-quality electron beam and to accelerate it by plasma wakefields to higher energies while preserving its initial quality. To the knowledge of the authors, only conventional accelerators, for example, LINACs, can provide to date low-energy spread (below the percent level) electron beams also with stability in charge, pointing and energy fluctuations at the injection into the plasma wave. Therefore here, laser-plasma accelerated electron beams at the current stage are not considered for the external injection. The influence of the energy spread on the betatron radiation spectrum is that to modify the critical energy following Equation (12). As far as the changes in the ratio R_{cap}/r_0 are greater than the quantity $2d\gamma/\gamma$, the tuning is possible and effective. Actually, except for energy spreads of the order of 100% (or even greater) sometimes obtained in laser-plasma acceleration experiments, the tuning is practically not importantly limited by the energy spread of the electron beam. The tuning function of Fig. 9 shows that modifying the laser-capillary matching conditions can yield a tuning of the critical energy at the level of many tens of percent. Therefore at a good level of approximation Fig. 9 represents the expected result of betatron radiation tuning in an external injection based on our choice of parameters for laser, plasma and capillary waveguide.

V. CONCLUSIONS

The dynamics of electrons externally injected inside an electron plasma wave generated by a laser driver guided in a multimodal configuration into a capillary waveguide has been studied on the base of a laser propagation model, by which the plasma wakefields are calculated. The laser coupling to the capillary modes is determined by the choice of the capillary diameter size and material, by the size of the laser beam at the entrance of the capillary, and by the laser intensity and plasma density, in fact, the interaction between the laser pulse and the generated electron plasma wave can give rise to a further mode coupling mechanism. A specific balance of electromagnetic modes inside the capillary can be chosen by setting the initial laser, capillary, and plasma characteristics. To a specific balance of electromagnetic modes corresponds a specific structure of the wakefield along the capillary. The wakefield structure actually affects the electron dynamics, in particular, in the transverse plane where betatron oscillations occur due to the focusing plasma wakefields. The correlation between the electron transverse dynamics and the emitted radiation spectra reveals the possibility of tuning the radiation spectra by modifying the mixture of the laser modes co-propagating inside the capillary. By setting a specific mixture of modes inside the waveguide, the controlled tuning of the radiation spectra becomes possible. This effect could be both used as indirect diagnostics of the laser coupling inside the capillary and especially as tuning mechanism for the betatron oscillations meant as the underlying physical mechanism to design innovative X–γ ray secondary sources.[22]

ACKNOWLEDGMENTS

We acknowledge financial support from the MIUR grant Rita Levi Montalcini.

[1]A. Rousse, K. Ta Phuoc, R. Shah, A. Pukhov, E. Lefebvre, V. Malka, S. Kiselev, F. Burgy, J. Rousseau, D. Umstadter, and D. Hulin, Phys. Rev. Lett. **93**, 135005 (2004).
[2]S. Wang, C. E. Clayton, B. E. Blue, E. S. Dodd, K. A. Marsh, W. B. Mori, C. Joshi, S. Lee, P. Muggli, T. Katsouleas, F. J. Decker, M. J. Hogan, R. H. Iverson, P. Raimondi, D. Walz, R. Siemann, and R. Assmann, Phys. Rev. Lett. **88**(13), 135004 (2002).
[3]E. Esarey, B. A. Shadwick, P. Catravas, and W. P. Leemans, Phys. Rev. E **65**, 056505 (2002).
[4]S. Kneip, C. McGuffey, F. Dollar, M. S. Bloom, V. Chvykov, G. Kalintchenko, K. Krushelnick, A. Maksimchuk, S. P. D. Mangles, T. Matsuoka, Z. Najmudin, C. A. J. Palmer, J. Schreiber, W. Schumaker, A. G. R. Thomas, and V. Yanovsky, Appl. Phys. Lett. **99**(9), 093701 (2011).
[5]S. Fourmaux, S. Corde, K. Ta Phuoc, P. Lassonde, G. Lebrun, S. Payeur, F. Martin, S. Sebban, V. Malka, A. Rousse, and J. C. Kieffer, Opt. Lett. **36**(13), 2426–2428 (2011).
[6]S. Kneip, C. McGuffey, J. L. Martins, S. F. Martins, and Z. Najmudin, Nat. Phys. **6**(12), 980–983 (2010).
[7]K. T. Phuoc, R. Fitour, A. Tafzi, T. Garl, N. Artemiev, R. Shah, and A. Pukhov, Phys. Plasmas **14**(8), 080701 (2007).
[8]K. T. Phuoc, E. Esarey, V. Leurent, E. Cormier-Michel, C. G. R. Geddes, C. B. Schroeder, and W. P. Leemans, Phys. Plasmas **15**(6), 063102 (2008).
[9]B. Cros, C. Courtois, G. Matthieussent, A. Di Bernardo, D. Batani, N. Andreev, and S. Kuznetsov, Phys. Rev. E **65**(2), 026405 (2002).
[10]M. Veysman, N. E. Andreev, K. Cassou, Y. Ayoul, G. Maynard, and B. Cros, JOSA B **27**(7), 1400–1408 (2010).
[11]C. Courtois, A. Couairon, B. Cros, J. R. Marques, and G. Matthieussent, Phys. Plasmas **8**(7), 3445–3456 (2001).
[12]N. E. Andreev, B. Cros, L. M. Gorbunov, G. Matthieussent, P. Mora, and R. R. Ramazashvili, Phys. Plasmas **9**(9), 3999–4009 (2002).
[13]N. E. Andreev, B. Cros, G. Maynard, P. Mora, and F. Wojda, IEEE Trans. Plasma Sci. **36**(4), 1746 (2008).
[14]B. S. Paradkar, B. Cros, P. Mora, and G. Maynard, Phys. Plasmas **20**(8), 083120 (2013).
[15]J. Ju, K. Svensson, H. Ferrari, A. Döpp, G. Genoud, F. Wojda, and B. Cros, Phys. Plasmas **20**(8), 083106 (2013).
[16]A. R. Rossi, A. Bacci, M. Belleveglia, E. Chiadroni, A. Cianchi, G. Di Pirro, and A. Mostacci, Nucl. Instrum. Methods A **740**, 60–66 (2014).
[17]A. Curcio, M. Petrarca, D. Giulietti, and M. Ferrario, Opt. Lett. **41**(18), 4233–4236 (2016).
[18]E. Esarey, C. B. Schroeder, and W. P. Leemans, Rev. Mod. Phys. **81**(3), 1229 (2009).
[19]J. T. Mendonça, Plasma Phys. Controlled Fusion **51**(2), 024007 (2009).
[20]A. Curcio, D. Giulietti, G. Dattoli, and M. Ferrario, J. Plasma Phys. **81**(5), 495810513 (2015).
[21]L. D. Landau and E. M. Lifshtiz, *The Classical Theory of Fields* (Pergamon Press, 1971).
[22]A. Curcio and D. Giulietti, Nucl. Instrum. Methods, B **355**, 214–216 (2015).